INTERNATIONAL JOURNAL FOR NUMERICAL METHODS IN ENGINEERING, VOL. 41, 541–558 (1998)

ANALYSIS OF SHELL-LIKE STRUCTURES BY THE BOUNDARY ELEMENT METHOD BASED ON 3-D ELASTICITY: FORMULATION AND VERIFICATION

YIJUN LIU*

Department of Mechanical Engineering, University of Cincinnati, P.O. Box 210072, Cincinnati, OH 45221-0072, U.S.A.

ABSTRACT

In this paper, the Boundary Element Method (BEM) for 3-D elastostatic problems is studied for the analysis of shell or shell-like structures. It is shown that the conventional boundary integral equation (CBIE) for 3-D elasticity does not degenerate when applied to shell-like structures, contrary to the case when it is applied to crack-like problems where it does degenerate due to the closeness of the two crack surfaces. The treatment of the nearly singular integrals, which is a crucial step in the applications of BIEs to thin shapes, is presented in detail. To verify the theory, numerical examples of spherical and ellipsoidal vessels are presented using the BEM approach developed in this paper. It is found that the system of equations using the CBIE is well conditioned for all the thickness studied for the vessels. The advantages, disadvantages and potential applications of the proposed BEM approach to shell-like structures, as compared with the FEM regarding modelling and accuracy, are discussed in the last section. Applications of this BEM approach to shell-like structures with non-uniform thickness, stiffeners and layers will be reported in a subsequent paper. © 1998 John Wiley & Sons, Ltd.

Int. J. Numer. Meth. Engng., **41**, 541–558 (1998)

KEY WORDS: shell-like structures; boundary element method; 3-D elasticity

1. INTRODUCTION

Accurate and reliable numerical analysis of plate and shell structures has been one of the challenging tasks for the computational mechanics. The Finite Element Method (FEM) has been a successful tool for the analysis of plate and shell structures in most applications. FEM is versatile and widely applied in engineering in the analysis of plate and shell structures. However, plate and shell theories are based on various assumptions about the geometry, loading and deformation of the structure. The plate or shell finite elements based on these theories, therefore, have many limitations in applications, such as numerical locking, edge effect, length scaling and especially the convergence problem (the FEM may not converge or converge to wrong answers under certain conditions), see, e.g. References 1–4. A great deal of research effort has been made in the last three decades in the FEM plate and shell analysis, to adjust the various assumptions in the theories, to improve the accuracy by using higher-order elements, to take account of more complex geometry of real structures, and so on. Still, the FEM modelling and analysis of shell-like

*Correspondence to: Yijun Liu, Department of Mechanical Engineering, University of Cincinnati, P.O. Box 210072, Cincinnati, OH 45221-0072, U.S.A.

CCC 0029–5981/98/030541–18$17.50 *Received 5 May 1997*
© 1998 John Wiley & Sons, Ltd.

structures in engineering applications are very delicate and demanding. It is often difficult, and even impractical, for structural analysis engineers to distinguish among thin shell, thick shell and 3-D elasticity models, and then choose the right type of finite elements accordingly in the analyses of a complicated structure. This is especially true during the structure design process when the dimensions (e.g. thickness) of a complicated structure endure changes from one design iteration to another.

The Boundary Element Method (BEM) for the analysis of plates and shells has been investigated intensively for both linear and non-linear problems for the last two decades (see, e.g. References 5–8 on plates, and a comprehensive review on shells[9] and the references therein). As in the case of the finite element method, these BEM formulations of plate and shell problems are based on the various plate and shell theories as well. Therefore, their applications are limited to cases of simple geometry or loading conditions. For example, the thickness of the plate or shell in these BEM models is required, in general, to be uniform. The fundamental solutions that are essential to the BEM are not readily available for some complicated shell structures. Another important factor is that BEM based on plate and shell theories uses 1-D (line) elements on the edges of the plate or shell. This is an advantage regarding the dimension reduction of the problems, but makes it difficult to couple with other BEM equations, which are discretized on the surfaces of structures, e.g. in the analyses of fluid–structure interactions.

In view of the above observations, it is advantageous and certainly on a solid theoretical ground to turn to 3-D elasticity theory in building numerical models for plate- and shell-like structures. With the rapid increase of the computing power, this is feasible now and may be the preferred method in the future for solving plate- and shell-like problems, at least when high accuracy is demanded, as discussed in Reference 2. Because of its features of the surface discretization and high accuracy, the BEM is in general preferred to the FEM in the realm of 3-D structural analysis, especially for the stress analysis. All these considerations prompted the study of using the BEM based on 3-D elasticity theory in the analysis of shell-like structures.

There are two major difficulties when the commonly used boundary integral equations (BIEs) are applied directly to thin-body problems (including thin voids or open cracks, thin shell-like structures and thin layered structures), where two parts of the boundary become close to each other; see References 10 and 11. One difficulty is the degeneracy of the linear systems of equations generated from the BIEs. The other is the difficulty of nearly singular integrals which arise in such problems. Because of these two difficulties, for a long time the BEM has been considered not suitable for thin-body problems. Recent progresses in References 10–14 have shown that the two difficulties can be overcome readily with some analytical effort. In Reference 10, the BIE formulations for thin body problems, specifically, for thin (rigid and soft) inclusions in acoustic medium, are constructed using a combination of the conventional BIE (CBIE) and the hypersingular BIE—the derivative of the CBIE. It is shown that this combined BIE formulation for the *exterior* domain will not degenerate no matter how thin the inclusions are. This is a general approach and can provide stable BIE formulations for the analysis of thin-body problems. An application of this approach to the scattering of elastic waves from open cracks is discussed in Reference 15. However, all these research efforts have focused on the degeneracy issue of the BIE for *exterior* type of problems, such as thin inclusions, voids or open cracks in structures. Whether the CBIE will degenerate or not for *interior*-type problems, such as thin shell-like structures, is not clear and has not been addressed in the BEM literature.

In this paper, it is established that the conventional BIE formulation for 3-D elasticity problems will not degenerate when applied to shell-like structures, contrary to the case when it is

 © 1998 John Wiley & Sons, Ltd.

applied to crack-like problems where it does degenerate, due to the closeness of the two surfaces in the structures. This assertion will be verified both analytically and numerically. A careful analysis of the limiting process as the two surfaces approaching each other reveals that the two equations from the CBIE collocated on the two surfaces are *independent* for shell-like structures, while *dependent* for crack-like problems (which is well known in the BEM literature). The treatment of the nearly singular integrals in the CBIE for 3-D elastostatic problems is presented in detail using a line integral approach. For the numerical verification of the theory, two test problems using a spherical and an ellipsoidal vessels are studied applying the BEM approach. It is found that the system of equations using the CBIE is well conditioned (thus non-degenerate) for all the values of thickness studied for the vessels. The advantages, disadvantages and potential applications of the proposed BEM approach to shell-like structures, as compared with the FEM regarding modelling efficiency and analysis accuracy, are discussed in the last section. Applications of this BEM approach to shell-like structures with non-uniform thickness, stiffeners and layers will be reported in a subsequent paper.

2. NON-DEGENERACY OF THE CONVENTIONAL BIE FOR SHELL-LIKE STRUCTURES

Consider the following conventional boundary integral equation (CBIE) for 3-D elastostatic problems [16–18] (index notation is used in this paper),

$$\frac{1}{2}u_i(P_o) = \int_S [U_{ij}(P, P_o)t_j(P) - T_{ij}(P, P_o)u_j(P)]\,\mathrm{d}S(P), \quad \forall P_o \in S \tag{1}$$

where u_i and t_i are the displacement and traction fields, respectively, U_{ij} and T_{ij} the displacement and traction kernels (Kelvin's solution), respectively, P the field point, P_o the source point and S the boundary surface of the structure. Sufficient smoothness of S at the source point P_o is assumed in equation (1), otherwise the coefficient $\frac{1}{2}$ will be replaced by a different number. CBIE (1) contains a singular integral of the Cauchy principle value (CPV) type, which, in general, demands delicate numerical quadratures. This CPV integral, however, can be removed from the CBIE by recasting it in a weakly singular form which should be used for the discretization of the CBIE (see e.g. References 18–21). The singular form of the CBIE, as given by equation (1), is only used in this paper for the purpose of discussion of the degeneracy of the CBIE for thin shapes.

To simplify the discussion hereafter, the following integral operator notation is introduced:

$$B[\bullet] = \int_S \mathbf{U}(P, P_o)[\bullet]\,\mathrm{d}S, \quad D[\bullet] = \int_S \mathbf{T}(P, P_o)[\bullet]\,\mathrm{d}S \tag{2}$$

where $\mathbf{U} = [U_{ij}]$ and $\mathbf{T} = [T_{ij}]$ are two 3×3 matrices for the kernels. Notice that the two integrals represented in (2) are corresponding to the single-layer and double-layer integrals, respectively, in the classical potential theory. Equation (1) can be, therefore, written as

$$\tfrac{1}{2}\mathbf{u} = B\mathbf{t} - D\mathbf{u} \tag{3}$$

where $\mathbf{u}$ and $\mathbf{t}$ are the displacement and traction vectors, respectively.

Without loss of generality, assume that S is the boundary of a thin shape in the structure (e.g. a void or a shell-like structure) and $S = S^+ \cup S^-$, with S^+ and S^- being the two separate surfaces for the thin shape and h a characteristic thickness of the thin shape; see Figure 1. Then equation

© 1998 John Wiley & Sons, Ltd.

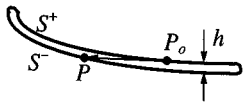

Figure 1. The boundary S of a thin shape: $S = S^+ + S^-$

(1) or (3) can be rewritten as follows, according to the position of the source point P_o:

$$\tfrac{1}{2}\mathbf{u}^+ = B_+^+\mathbf{t}^+ - D_+^+\mathbf{u}^+ + \mathrm{B}_-^+\mathbf{t}^- - D_-^+\mathbf{u}^-, \quad \forall P_o \in S^+ \tag{4}$$

and

$$\tfrac{1}{2}\mathbf{u}^- = \mathbf{B}_+^-\mathbf{t}^+ - D_+^-\mathbf{u}^+ + B_-^-\mathbf{t}^- - D_-^-\mathbf{u}^-, \quad \forall P_o \in S^- \tag{5}$$

where the superscripts for the **u** and **t** vectors indicate the surface (S^+ or S^-) on which they are evaluated; superscripts for the two integral operators B and D indicate the location of P_o and the subscripts indicate the surface of integration. For example,

$$\mathbf{u}^+ \equiv \mathbf{u}(P_o), \quad \forall P_o \in S^+$$

$$B_+^+[\bullet] \equiv \int_{S^+} \mathbf{U}(P, P_o)[\bullet]\,\mathrm{d}S, \quad \forall P_o \in S^+$$

$$B_-^+[\bullet] \equiv \int_{S^-} \mathbf{U}(P, P_o)[\bullet]\,\mathrm{d}S, \quad \forall P_o \in S^+$$

It is well known that the CBIE (1) will degenerate for crack problems, i.e. the equation generated on one surface of a crack will be identical to that generated on the opposite surface (see, e.g. References 10 and 22). CBIE alone is, therefore, insufficient in solving crack or crack-like problems in a general setting. However, whether CBIE will degenerate or not for thin shell-like structures is not clear in the BEM literature. The general consensus in the BEM community is that the CBIE, if not all types of BIEs, should not be applied to thin bodies or shell-like structures, due to the (possible) degeneracy of the CBIE formulation and the difficulty of dealing with the nearly singular integrals encountered in thin-body problems. In this section, the issue of degeneracy of the CBIE for crack-like problems is revisited, followed by an investigation of the degeneracy of the CBIE for shell-like problems. The nearly singular integrals will be discussed in detail in the next section.

To study the behaviour of the CBIE when the thickness h of a thin shape approaches zero (Figure 1), it is necessary to consider the two cases (crack-like or shell-like problems) separately, which demonstrate totally different characteristics regarding the degeneracy of the CBIE.

2.1. Case 1. Exterior-like problem

In this case, the material or problem domain is *outside* of the surface $S = S^+ \cup S^-$, and the outward normal (n^+ on S^+ and n^- on S^-) is pointing in the way as shown in Figure 2. Voids or open cracks in structures are some examples in this case.

 © 1998 John Wiley & Sons, Ltd.

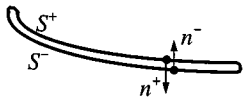

Figure 2. The boundary and normal for an *exterior* problem (a void or crack in solids)

In the limit that S^- tends to S^+, or equivalently, h tends to zero (Figures 1 and 2), the following limits of the integrals in (4) and (5) exit:

$$B_-^+, B_-^-, B_+^- \to B^+ \tag{6}$$

$$D_-^+ \to \tfrac{1}{2}I - D^+, \quad D_-^- \to -D^+, \quad D_+^- \to \tfrac{1}{2}I + D^+ \tag{7}$$

where $B^+ \equiv B_+^+$, $D^+ \equiv D_+^+$ for brevity, and I is the identity operator. The limits in (6) are obvious since the U_{ij} kernel is symmetric for S^+ and S^-, and there is no jump terms for the single-layer integral represented by B in (2). The limits in (7) are more delicate since the T_{ij} kernel is antisymmetric on S^+ and S^- (i.e. $T_{ij}^+ = -T_{ij}^-$), and there is a jump term for the double-layer integral D. The sign of the jump term ($\frac{1}{2}I$) is related to the direction of the normal which, in this case, is pointing to the opposite of the direction along which P_o is approaching the opposite surface. For example, the first limit in (7) is derived by

$$\begin{aligned}
\lim_{S^- \to S^+} (D_-^+ \mathbf{u}^-) &= \lim_{S^- \to S^+} \int_{S^-} T_{ij}(P, P_o) u_j^-(P)\, \mathrm{d}S(P) \quad (\text{with } P_o \in S^+) \\
&= \lim_{P_o \to S^-} \int_{S^-} T_{ij}(P, P_o) u_j^-(P)\, \mathrm{d}S(P) \\
&= \frac{1}{2} u_i^-(P_o) + \int_{S^-} T_{ij}(P, P_o) u_j^-(P)\, \mathrm{d}S(P) \quad (\text{CPV}) \\
&= \frac{1}{2} u_i^-(P_o) - \int_{S^+} T_{ij}(P, P_o) u_j^-(P)\, \mathrm{d}S(P) \quad (\text{CPV})
\end{aligned}$$

i.e.

$$D_-^+ \mathbf{u}^- \to (\tfrac{1}{2}I - D^+)\mathbf{u}^-$$

This leads to the first result in (7). Notice that $D^+\mathbf{u}^-$ is a CPV-type integral after the limit has been taken.

Considering the limit as $h \to 0$ for equations (4) and (5), and applying the results in (6) and (7), one has the following two limiting equations generated by placing P_o on S^+ and S^-, respectively,

$$\tfrac{1}{2}\mathbf{u}^+ = B^+\mathbf{t}^+ - D^+\mathbf{u}^+ + B^+\mathbf{t}^- - (\tfrac{1}{2}I - D^+)\mathbf{u}^- \quad \text{from } P_o \in S^+$$

and

$$\tfrac{1}{2}\mathbf{u}^- = B^+\mathbf{t}^+ - (\tfrac{1}{2}I + D^+)\mathbf{u}^+ + B^+\mathbf{t}^- - (-D^+)\mathbf{u}^- \quad \text{from } P_o \in S^-$$

© 1998 John Wiley & Sons, Ltd.

The above two equations are identical and can be written as

$$D^+\Delta\mathbf{u} + \tfrac{1}{2}\Sigma\mathbf{u} = B^+\Sigma\mathbf{t} \tag{8}$$

where $\Delta\mathbf{u} = \mathbf{u}^+ - \mathbf{u}^-$, $\Sigma\mathbf{u} = \mathbf{u}^+ + \mathbf{u}^-$, and $\Sigma\mathbf{t} = \mathbf{t}^+ + \mathbf{t}^-$. This reveals that the CBIE for crack or crack-like problems is *degenerate* due to the fact that the two equations from both sides of the crack are reduced to one. The remaining equation after the limiting process, i.e. equation (8), is insufficient in determining all the unknowns ($\Sigma\mathbf{u}$ and $\Delta\mathbf{u}$ across the crack, or $\mathbf{u}$ on the two surfaces). The remedy to this degeneracy is either to avoid it by using the multi-region BIE approach[22] in some cases or to employ the hypersingular BIEs.[10,15,23–25]

2.2. Case 2. Interior-like problem

In this case, the material or problem domain is *inside* of the surface $S = S^+ \cup S^-$, and the outward normal is pointing in the way as shown in Figure 3. Shells or shell-like structures are some examples in this case.

In the limit that S^- tends to S^+, or h tends to zero (Figures 1 and 3), one can obtain the following limits of the integrals in (4) and (5):

$$B^+_-, B^-_-, B^-_+ \to B^+ \tag{9}$$

$$D^+_- \to -\tfrac{1}{2}I - D^+, \quad D^-_- \to -D^+, \quad D^-_+ \to -\tfrac{1}{2}I + D^+ \tag{10}$$

where, as earlier, $B^+ \equiv B^+_+$, $D^+ \equiv D^+_+$, and I is the identity operator. The limits in (9) are the same as in (6) since the U_{ij} kernel is not related to the normal. The limits in (10) are different from their corresponding limits in (7) only in the sign of the jump terms, which is due to the change of the direction of the normal. For interior-like problems, the direction of the normal of the integration surface is pointing to the same direction in which P_o is approaching to this surface.

Considering the limit as $h \to 0$ in equations (4) and (5), and applying the results in (9) and (10), one has the following two limiting equations for the interior-like regions:

$$\tfrac{1}{2}\mathbf{u}^+ = B^+\mathbf{t}^+ - D^+\mathbf{u}^+ + B^+\mathbf{t}^- - (-\tfrac{1}{2}I - D^+)\mathbf{u}^- \quad \text{from } P_o \in S^+$$

and

$$\tfrac{1}{2}\mathbf{u}^- = B^+\mathbf{t}^+ - (-\tfrac{1}{2}I + D^+)\mathbf{u}^+ + B^+\mathbf{t}^- - (-D^+)\mathbf{u}^- \quad \text{from } P_o \in S^-$$

The above two equations can be rewritten as

$$(D^+ + \tfrac{1}{2}I)\Delta\mathbf{u} = B^+\Sigma\mathbf{t}, \quad P_o \in S^+ \tag{11}$$

and

$$(D^+ - \tfrac{1}{2}I)\Delta\mathbf{u} = B^+\Sigma\mathbf{t}, \quad P_o \in S^- \tag{12}$$

respectively, where $\Delta\mathbf{u} = \mathbf{u}^+ - \mathbf{u}^-$ and $\Sigma\mathbf{t} = \mathbf{t}^+ + \mathbf{t}^-$ as before.

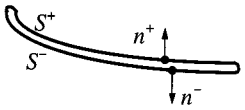

Figure 3. The boundary and normal for an *interior* problem (shell-like structures)

 © 1998 John Wiley & Sons, Ltd.

Equations (11) and (12) are two distinct or linearly independent equations which can be combined in the following matrix form involving the original boundary variables **u** and **t**:

$$\begin{bmatrix} (D^+ + \frac{1}{2}I) & -(D^+ + \frac{1}{2}I) \\ (D^+ - \frac{1}{2}I) & -(D^+ - \frac{1}{2}I) \end{bmatrix} \begin{Bmatrix} \mathbf{u}^+ \\ \mathbf{u}^- \end{Bmatrix} = \begin{bmatrix} B^+ & B^+ \\ B^+ & B^+ \end{bmatrix} \begin{Bmatrix} \mathbf{t}^+ \\ \mathbf{t}^- \end{Bmatrix} \tag{13}$$

In theory, equation (13) will degenerate if the displacement boundary condition is imposed *everywhere*, which leads to the situation of solving for the unknown traction **t** using the matrix on the right-hand side of (13). For example, if $\mathbf{u}^+ = \mathbf{u}^- = \bar{\mathbf{u}}$ everywhere, then $\Delta\mathbf{u} = \mathbf{0}$, and equations (11) and (12) will become identical, hence equation (13) or CBIE is degenerate. Another situation is that the thickness h of the shell or shell-like structure is approaching zero which leads to $\mathbf{u}^+ = \mathbf{u}^-$ and hence $\Delta\mathbf{u} = \mathbf{0}$. However, both of these scenarios are unlikely to happen in real structural analysis problems. In a general stress analysis problem, the displacements are described on only part of the boundary and forces on the remaining part. The coefficient matrix for the unknowns is a mix of the matrices on both sides of equations (11) and (12). This arrangement makes the two equations remain distinctive from each other. On the other hand, as long as the thickness h of the shell or shell-like structure is finite, and $\mathbf{u}^+$ and $\mathbf{u}^-$ are identified as independent variables, the characteristics of equation (13) will not change. In the case that h tends to zero, the fact that $\mathbf{u}^+$ should approach $\mathbf{u}^-$ will come out of the solution of equation (13). The equation itself remains solvable in this case. Notice that for inclusion problems, such as shells surrounded by another media or thin layers in different materials, equation (13) is well-conditioned since in this case both **u** and **t** are unknowns. The non-degeneracy of the CBIE for an interior region in inclusion problems has been demonstrated in Reference 10 in the context of acoustic wave problems.

Based on the above analysis and justification, it is concluded that the CBIE will not degenerate for the analysis of shell or shell-like structures, if the structures are not constrained at *all* the boundaries (as they are in almost all the engineering applications). This is in contrast to the cases of crack or crack-like problems where the CBIE does degenerate. The remaining concerns with the applications of the CBIE to shell or shell-like structures are how to deal with the nearly singular integrals arising in such applications and what the advantages are when this BEM approach is compared with the finite element method. These issues are addressed in the following sections.

3. TREATMENT OF THE NEARLY SINGULAR INTEGRALS

In order to apply the CBIE (1) to shell-like structures, one has to overcome the difficulty of *near singularity* which arise when collocation point (source point P_o) is on one surface of the thin shell-like structure and integration need to be performed on the other nearby surface. Many numerical schemes for computing the nearly singular integrals can be found in the literature of the boundary element method, such as numerical integration with subdivisions, kernel cancellation method and the auxiliary surface method (see e.g. Reference 13 for a brief review). Among all the available methods, the line integral approach, i.e. transforming the nearly singular integral into a sum of weakly singular integrals and non-singular line integrals, seems to be one effective and efficient approach.[10,13] It is the method adopted and implemented in this study.

A typical nearly singular integral in equation (1) (CBIE) is the one with the stress kernel function T_{ij} and integrated on a surface ΔS with source point P_o nearby (Figure 4). Here ΔS can

© 1998 John Wiley & Sons, Ltd.

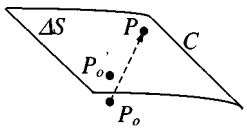

Figure 4. Source point P_o near the surface ΔS of integration

be one element or several elements on the surface S. This nearly singular integral can be dealt with by adding and subtracting a term in the following manner:

$$\int_{\Delta S} T_{ij}(P,P_o)u_j(P)\,\mathrm{d}S(P) = \int_{\Delta S} T_{ij}(P,P_o)\,[u_j(P)-u_j(P_o')]\,\mathrm{d}S(P) + u_j(P_o')\int_{\Delta S} T_{ij}(P,P_o)\,\mathrm{d}S(P) \tag{14}$$

where P_o' is the closest point on ΔS to P_o (an image point of P_o on ΔS); see Figure 4. The first integral is now at most nearly weakly singular and can be computed using the conventional quadratures. The last integral in (14) can be transformed into line integrals as follows by using the Stokes' theorem:[13]

$$\int_{\Delta S} T_{ij}(P,P_o)\,\mathrm{d}S(P) = I_\Omega(P_o)\delta_{ij} + \frac{1}{4\pi}\varepsilon_{ijk}\oint_C \frac{1}{r}\mathrm{d}x_k + \frac{1}{8\pi(1-\nu)}\varepsilon_{jkl}\oint_C r_{,ik}\,\mathrm{d}x_l \tag{15}$$

where C is the boundary curve of ΔS, $r = |P_oP|$, ν the Poisson's ratio, ε_{ijk} the permutation tensor and

$$I_\Omega(P_o) = \int_{\Delta S}\frac{\partial G}{\partial n}\,\mathrm{d}S = -\frac{1}{4\pi}\int_{\Delta S}\frac{1}{r^2}\frac{\partial r}{\partial n}\,\mathrm{d}S$$

is a solid angle integral ($G = 1/4\pi r$ is the Green's function for potential problems). This surface integral can also be evaluated using a line integral. This needs more explanation that is not furnished in Reference 13.

Consider a local co-ordinate system $Oxyz$ with the origin at the source point P_o and oriented in such a way that $+z$-axis passes through the surface ΔS; see Figure 5. Introducing the spherical co-ordinates (r, θ, φ), one can write the projection of the differential area $\mathrm{d}S$ on the sphere of radius r as

$$(\hat{r}\cdot\hat{n})\,\mathrm{d}S = r^2\sin\varphi\;\mathrm{d}\varphi\,\mathrm{d}\theta$$

where $\hat{r}$ is a unit vector along the $\mathbf{r}$ direction and $\hat{n}$ a unit vector along the normal direction. Since $\partial r/\partial n = (\hat{r}\cdot\hat{n})$, the solid angle integral can be evaluated as follows:

$$I_\Omega(P_o) = -\frac{1}{4\pi}\int_{\Delta S}\frac{1}{r^2}(\hat{r}\cdot\hat{n})\,\mathrm{d}S = -\frac{1}{4\pi}\int_0^{2\pi}\left[\int_0^{\Phi(\theta)}\sin\varphi\,\mathrm{d}\varphi\right]\mathrm{d}\theta = \frac{1}{4\pi}\int_0^{2\pi}[\cos\Phi(\theta)-1]\,\mathrm{d}\theta \tag{16}$$

 © 1998 John Wiley & Sons, Ltd.

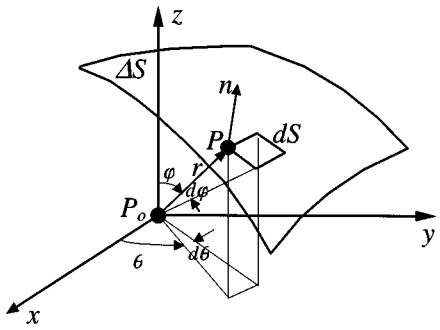

Figure 5. The solid angle integral

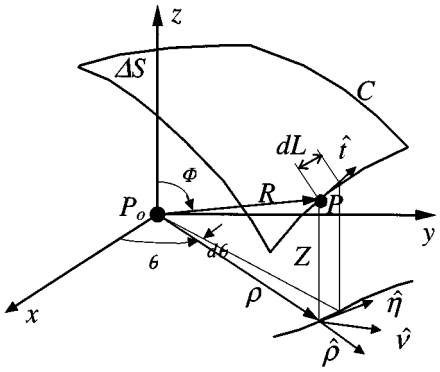

Figure 6. Geometry on the edge

where $\Phi(\theta)$ is the value of φ evaluated at the edge of ΔS. This is a 1-D integral with integrand evaluated on the contour C. Notice that if ΔS is a semi-sphere with its edge resting on the xy plane, then the solid angle integral is $-\frac{1}{2}$ by using (16), which is the number one finds in the BEM literature. To further convert the integral in (16) into an explicit form of line integrals, refer to Figure 6 and note the following relationships:

$$\rho \, \mathrm{d}\theta = (\hat{\rho} \cdot \hat{v})(\hat{t} \cdot \hat{\eta}) \, \mathrm{d}L \quad \text{and} \quad \cos \Phi(\theta) = \frac{Z(\theta)}{R(\theta)}$$

where R and Z are the two spherical co-ordinates of the point P on contour C, $\boldsymbol{\rho}$ the projection vector of $\mathbf{R}$ on the xy-plane, $\hat{\rho}$ the unit vector along $\boldsymbol{\rho}$; $\hat{t}$ and $\hat{\eta}$ are the (unit) tangential vectors of the contour C and the projection curve of C on xy-plane, respectively, and finally, $\hat{v} = \hat{\eta} \times \hat{z}$ with $\hat{z}$ being a unit vector along the z-axis. Thus, (16) can be converted readily into a line integral on contour C

$$I_\Omega(P_o) = \frac{1}{4\pi} \oint_C \left[\frac{Z(L)}{R(L)} - 1 \right] \frac{(\hat{\rho} \cdot \hat{v})(\hat{t} \cdot \hat{\eta})}{\rho} \, \mathrm{d}L \tag{17}$$

© 1998 John Wiley & Sons, Ltd.

All the line integrals in (15) and (17) are non-singular at all since the source point P_o is always off the contour C. This line integral approach for dealing with the nearly singular integrals is very efficient in computation. One does not need to use more elements in the model or subdivisions on an element in order to handle these nearly singular integrals. It is found that the CPU time used to compute the nearly singular integrals using this line integral approach is only a fraction of that used for applying many subdivisions on the original surface elements, when the same accuracy is achieved.

4. NUMERICAL VERIFICATION

To verify the theory on the non-degeneracy of the conventional BIE for thin shell-like structures, two simple test problems are studied where the BEM solutions are compared with the exact solution (if it is available) and the FEM solutions.

4.1. Test problem 1. A spherical vessel

First, a spherical shell-like vessel under internal pressure p shown in Figure 7 is studied. The inner radius a of the vessel is constant in this study, while the outer radius b changes from $1{\cdot}01a$ to $2a$. This setup, therefore, provides a model of the spherical vessel which can be categorized as a thin shell, a thick shell and eventually a bulky solid, according to the values of the ratio of b/a.

In the BEM model, both the inner and outer surfaces are discretized with 48 quadratic boundary elements (a total of 96 elements), with each octant having six elements on one surface as shown in Figure 8. Figure 9 shows the radial displacement at the inner surface using the BEM without the line integrals for the nearly singular integrals. The BEM solutions deteriorate when the two surfaces become closer (the ratio of b/a is below $1{\cdot}1$), as expected. The BEM results improve dramatically when the line integrals are employed for the nearly singular integrals, as shown in Figure 10. Figure 11 is a plot of the hoop (tangential) stress at the inner surface using the BEM with line integrals, which is also in good agreement with the analytical solution. The system of equations using the CBIE is well-conditioned even when the thickness of the shell is only $1 \sim 5$ percent of the inner radius of the sphere ($b/a = 1{\cdot}01 \sim 1{\cdot}05$). Earlier studies have shown that near or below this range of the thinness for a thin shape, the CBIEs for a open crack or a rigid screen in acoustic medium degenerate as indicated by a large condition number for the system of

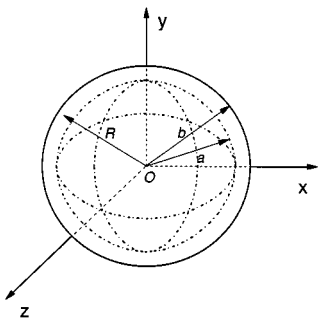

Figure 7. A spherical vessel under internal pressure p (inner radius $= a$, outer radius $= b$, Poisson's ratio $\nu = 0{\cdot}3$)

 © 1998 John Wiley & Sons, Ltd.

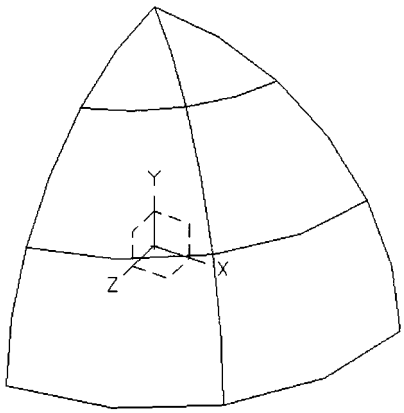

Figure 8. Mesh pattern for the boundary element analysis (total of 96 boundary elements on the two surfaces)

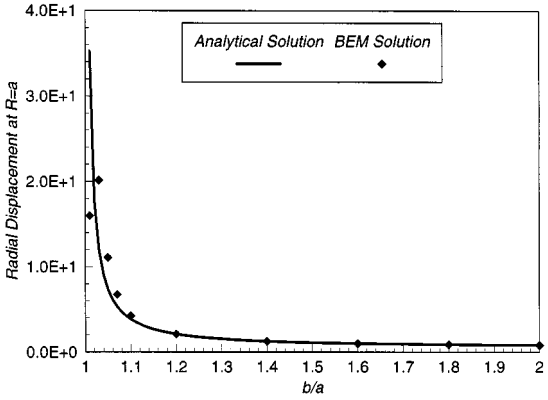

Figure 9. BEM solution of the radial displacement *without* using the line integrals for nearly singular integrals

equations.[10,15] In this study, however, further decrease of the shell thickness (to $b/a = 1{\cdot}005$) does not show any sign of degeneracy of the system of equations. The condition numbers stay below a few thousands. This simple example, therefore, supports the claim that the conventional BIE does not degenerate for thin shell-like structures as long as the nearly singular integrals are properly handled.

The finite element method is applied to this simple structure to investigate how the FEM handles the transitions of the structure from thin shell to thick shell, and finally to bulky solid. The mesh pattern in the first octant for the parabolic shell elements (6-node triangle and 8-node quadrilateral) used is shown in Figure 12. This mesh gives the same total number of elements and comparable accuracy as in BEM analysis. The second-order solid elements used have the same pattern as the shell elements, with one or two layers of elements in the radial direction. Figure 13 is a comparison of the BEM and FEM for the stress calculation. In the FEM approach, the shell model is applied when $1{\cdot}01 \leqslant b/a \leqslant 1{\cdot}1$, while the solid model is used when $1{\cdot}1 \leqslant b/a \leqslant 2{\cdot}0$. The *SDRC/I-DEAS Master Series/Simulation* module is used for this finite element analysis. As shown

© 1998 John Wiley & Sons, Ltd.

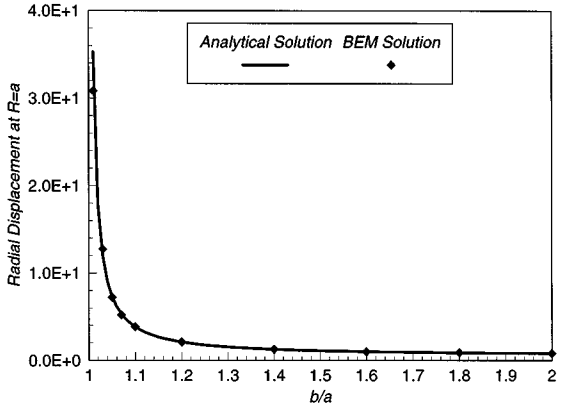

Figure 10. BEM solution of the radial displacement using the line integrals for nearly singular integrals

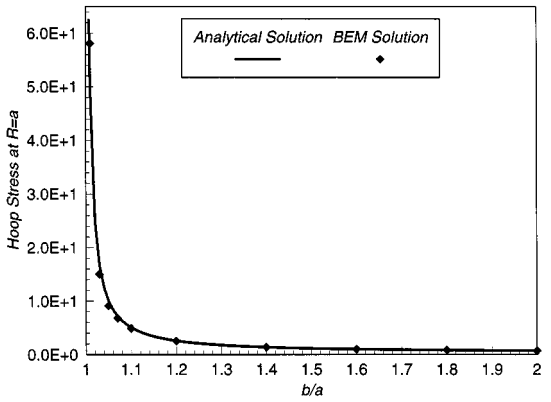

Figure 11. BEM solution of the hoop stress using the line integrals for nearly singular integrals

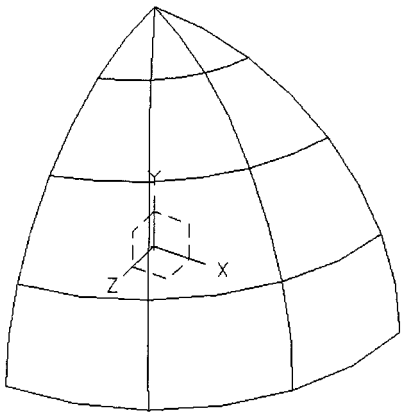

Figure 12. Mesh pattern for the finite element analysis

 © 1998 John Wiley & Sons, Ltd.

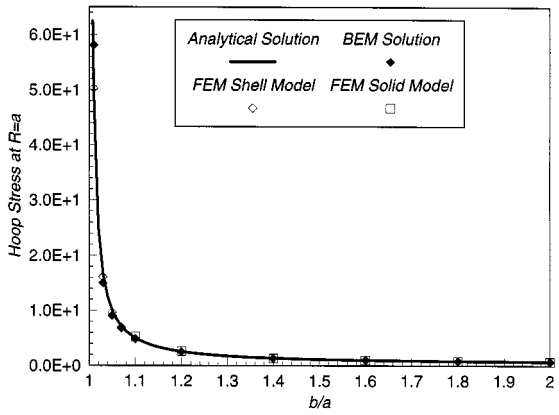

Figure 13. Comparison of the BEM and FEM (shell and solid elements) solutions for the hoop stress ($\times p$)

in Figure 13, the FEM results are in very good agreement with the exact solution for this simple problem. The only disadvantage of the FEM in this analysis is the need of different models (shell and solid) and re-meshing in the solid model when the thickness of the vessel is changing dramatically. On the other hand, in the BEM approach, only one model (BEM for 3-D elasticity) is used and no need to re-mesh as the thickness changes.

4.2. Test problem 2. An 'ellipsoidal vessel' with non-uniform thickness

In this test, the geometry of the spherical shell in the previous test is modified so that the outer surface becomes an ellipsoid (short axis $= c$ along the y-direction and long axis $= d$ along the x- and z-direction) and the inner surface remains a sphere (radius $= a$) (Figure 14). The ratio of d/a is fixed at 1·2 while the ratio of c/a is changed from 1·05, 1·03 to 1·01. These are simple cases of shell-like structures with *non-uniform* thickness, and present greater challenges to both the BEM and FEM due to the rapid variations in the stress fields. No analytical solution is found for this problem.

The hoop stresses at point A and point B (Figure 14) on the inner surface, using the BEM and FEM, are given in Table I. The total numbers of elements used in each mesh (for the whole structure) are listed in Table II for reference. Due to symmetry conditions, only one-eighth of the whole structure is used in the FEM analysis. Mesh 1 for the BEM has the same mesh pattern as shown in Figure 8, while Mesh 1 for the FEM has a similar mesh pattern to that shown in Figure 12 and has two layers of second-order solid elements in the radial direction. FEM shell elements are difficult to use for this problem, because of the non-uniform thickness. The meshes for both BEM and FEM are oriented in such a way that no triangular elements are present near points A and B to avoid possible spurious stress values on triangular elements. The BEM and FEM results agree reasonably well for the first two cases ($c/a = 1{\cdot}05$ and 1·03) as the number of elements increases. Results for the last case ($c/a = 1{\cdot}01$) are not converged at point A using both BEM and FEM. It is found that in this extreme case the results are very sensitive to the meshes used in the FEM because of the small thickness near point A. No finer mesh is attempted for this case since further understanding of the behavior of such shell-like structures is deemed desirable.

© 1998 John Wiley & Sons, Ltd.

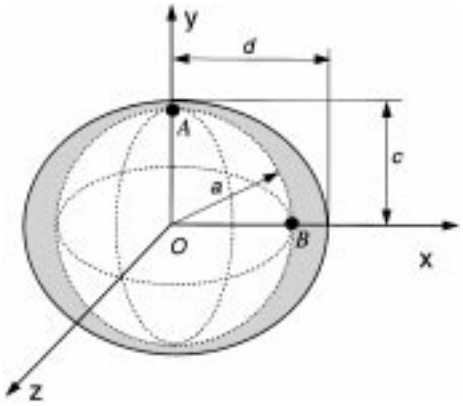

Figure 14. An 'ellipsoidal vessel' with non-uniform thickness and under internal pressure p (Poisson's ratio $v = 0{\cdot}3$, Young's modulus E)

Table I. Hoop stresses in the 'ellipsoidal vessel' ($\times p$). ($d/a = 1{\cdot}2$)

Ratio c/a	Mesh used	At point A		At Point B	
		BEM	FEM	BEM	FEM
1·05	1	8·724	11·048	1·938	3·152
	2	9·814	10·196	2·832	3·086
	3	10·226	9·451	2·920	3·077
1·03	1	11·723	18·067	1·800	3·191
	2	14·163	17·970	2·891	3·167
	3	15·544	15·691	2·976	3·164
1·01	1	16·952	39·247	1·224	3·155
	2	27·794	56·985	2·903	3·248
	3	35·098	46·978	3·145	3·258

Table II. Total number of elements used in each mesh

Mesh	BEM	FEM
1	96	192
2	192	768
3	384	5120

Note that stress results at point B are converged quickly and do not change significantly as the ratio of c/a decreases, which agrees with the intuition.

As is shown by the results in Table I, more elements are needed in FEM in order to obtain the accuracy and avoid very thin solid elements (with large aspect ratios) which can cause numerical

 © 1998 John Wiley & Sons, Ltd.

instability in the FEM. On the other hand, this test problem does not present any new difficulties in the modelling and analysis to the BEM approach, except for the fact that more elements are needed to account for the increased variations of the stress fields.

The two examples studied in this section are very simple ones in shell structures. The purpose of using these examples is to verify the non-degeneracy of the CBIE for shell-like structures. Studies of more complicated shell or shell-like structures, such as shells with non-uniform thickness and stiffeners, and layered shell structures, are underway. More delicate comparisons of the BEM and FEM for the analysis of such structures will also be carried out. All these will be reported in a subsequent paper.

5. DISCUSSIONS

The applicability of the conventional BIE for 3-D elasticity problems to the analysis of shell and shell-like structures is investigated in this paper. It is shown that the CBIE, with proper treatment of the nearly singular integrals, will not degenerate when it is applied to shell or shell-like structures, contrary to the case of a crack or thin void in structures, for which the CBIE does degenerate. The numerical verification using simple spherical and 'ellipsoidal vessel' models supports this assertion. The remaining questions are: What are the advantages of this BEM approach to the shell or shell-like structures? What are the potential applications of this approach?

Based on 3-D elasticity, the BEM approach presented in this paper can provide an alternative tool for the analysis of shell-like structures. Instead of identifying parts of a structure as plates, shells, or solids, this approach can treat the structure as a single elastic medium and model it continuously without the need to switch to different models. The FEM modelling and analysis of shell-like structures are very delicate and demanding in engineering practices. It is very difficult, and sometimes even impractical, to distinguish among the thin shell, thick shell and 3-D solid models and then to choose the finite element types accordingly. This is especially true during a structure design process where the dimensions (e.g. thickness) of a complex structure may change from one design iteration to another. Misuse of the plate and shell elements, in violations of their various assumptions, occurs quite often in engineering applications and leads to erroneous results. The BEM approach presented in this paper, using a continuous modelling concept, can eliminate all these hidden pitfalls in the applications and ensure simple modelling and accurate analyses for shell-like structures.

The modelling of the structure using the BEM is as easy as the FEM modelling using shell elements, since for the BEM only a surface mesh of the structure is needed. The BEM modelling will be much easier than the FEM modelling if solid finite elements are used, even with the widely available automatic meshing capabilities in various FEM packages. It was found that thin shapes (such as turbine blades, thin shells attached to bulky solids, etc.) can present great challenges to automatic meshers, which are often time-consuming and may provide undesirable mesh patterns or densities. Although two surfaces need to be modelled for a shell-like structure using the BEM, instead of one surface as in the FEM modelling using shell elements, less boundary elements can be used on each surface for a comparable accuracy, as is demonstrated in the examples in the previous section. On the other hand, each node in the BEM model has a fewer numbers of degree of freedom (DOF), or unknowns, than the numbers of DOF in FEM shell models where each node is associated with both translational and rotational DOFs. All these features of the BEM approach make it very attractive to the modelling and analysis of shell-like structures, besides the higher accuracy the BEM deliveries.

© 1998 John Wiley & Sons, Ltd.

The high accuracy of the boundary element method for stress analysis is well known, mainly due to its semi-analytical nature and surface-only discretization. This high accuracy will be retained in the analysis of shell-like structures using the BEM if the nearly singular integrals are computed accurately. There is, however, one major drawback regarding the computational efficiency of the proposed BEM approach. At present, the BEM is usually less efficient than the FEM in 3-D structural analysis, i.e. it takes longer to run a boundary element analysis. This is, in fact, a trade-off between human time and computer time, because significant manpower can be saved during the modelling stage when BEM is used for 3-D structures. In the future, this concern may become insignificant with the continued improvement in computer speeds. It is believed that future computational tools should be built on more accurate and solid theoretical foundations first, and the efficiency issues should be pursued later. Improvements in efficiency can always be achieved with the advance of computer technology, while improvements in accuracy are always limited by the theory on which the computational models are built.

Applications of the proposed BEM approach to shell-like structures can be found in many areas where the FEM approaches using the shell or solid elements are inefficient or inaccurate. Figure 15 shows the examples of some structures, such as thin-layered structures, turbine blades, rudders and various containers. All of these structures are shell-like structures, but cannot be analysed accurately using the traditional thin shell or thick shell finite elements. FEM using solid elements is accurate for such structures, but the finite element mesh is difficult to generate as discussed in the above. The proposed BEM approach is especially suited for the analysis of such shell-like structures, to provide means of simple modelling and high accuracy. In the sound-structure interaction area, the BEM is usually applied for the acoustic media and the FEM for the structures which, in many cases, are shell-like structures such as the various panels for a car body. Using the BEM approach for the structures can improve the accuracy and make a better coupling of the BEM equations from the structures and fluids in a coupled analysis. (The characteristics of FEM and BEM equations are drastically different, and a straightforward coupling of both is often awkward.) Finally, for the shape optimization of structures, the BEM is very appealing because of its boundary discretization nature and high accuracy in sensitivity analysis. The developed BEM approach can form the basis for the shape optimization analysis of shell-like structures.

Finally, it must be pointed out that the proposed BEM approach to shell-like structures should be considered as a complement to the FEM in the structural analysis. For structures that can be identified clearly as shells or bulky solids, the corresponding FEM should be used because of the efficiency FEM delivers. For shell-like structures where the shell models are inadequate and the

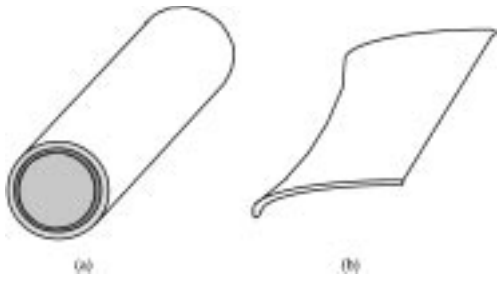

Figure 15. Shell-like structures: (a) layered structure; (b) thin structure with varying thickness (a blade)

 © 1998 John Wiley & Sons, Ltd.

solid models are difficult to obtain, the BEM approach can be used as an alternative, especially when high accuracy is desired, as in benchmarks.

ACKNOWLEDGEMENT

The author would like to thank Professor Frank Rizzo at Iowa State University and Dr. Guna Krishnasamy now at The MacNeal-Schwendler Corporation for many discussions on the subject of thin-bodies using the boundary element method. Their origination and effort have advanced the boundary element method to its full potential. Professor Rizzo's comments and suggestions on this manuscript are especially acknowledged. The author would also like to acknowledge the research startup fund from the University of Cincinnati, and the license of *SDRC/I-DEAS Master Series* from the Structural Dynamics Research Corporation.

REFERENCES

1. G. Wempner, 'Mechanics and finite elements of shells', *Appl. Mech. Rev.*, **42,** 129–142 (1989).
2. I. Babuska and J. T. Oden, 'Benchmark computation: What is its purpose and meaning?', *USACM Newslett.*, **5,** (1992).
3. J. R. Cho and T. T. Oden, '*A priori* error estimations of hp-finite element approximations for hierarchical models of plate- and shell-like structures', *Comput. Methods Appl. Mech. Engng.*, **132,** 135–177 (1996).
4. M. Bernadou, *Finite Element Methods for Thin Shell Problems*, Wiley, Chichester, 1996.
5. M. Stern, 'Boundary integral equations for bending of thin plates', in: C. A. Brebbia (ed.), *Progress in Boundary Elements*, Chap. 6, Vol. 2, Pentech Press, London, 1983.
6. T. Q. Ye and Y. J. Liu, 'Finite deflection analysis of elastic plate by the boundary element method', *Appl. Math. Modelling*, **9,** 183–188 (1985).
7. Y. J. Liu, 'Elastic stability analysis of thin plate by the boundary element method—a new formulation', *Engng. Anal. Boundary Elements*, **4,** 160–164 (1987).
8. T. Matsumoto, M. Tanaka and K. Hondoh, 'A new regularized boundary integral formulation for thin elastic plate bending analysis', in: C. A. Brebbia and G. S. Gipson (eds.), *Boundary Elements XIII*, Tulsa, OK, 1991, Computation Mechanics Publications, pp. 523–533.
9. D. E. Beskos, 'Static and dynamic analysis of shells', in D. E. Beskos (ed.), *Boundary Element Analysis of Plates and Shells*, Springer, Berlin, 1991, pp. 93–140.
10. G. Krishnasamy, F. J. Rizzo and Y. J. Liu, 'Boundary integral equations for thin bodies', *Int. J. Numer. Meth. Engng.*, **37,** 107–121 (1994).
11. R. Martinez, 'The thin-shape breakdown (TSB) of the Helmholtz integral equation', *J. Acoust. Soc. Am.*, **90,** 2728–2738 (1991).
12. G. Krishnasamy, F. J. Rizzo and Y. J. Liu, 'Scattering of acoustic and elastic waves by crack-like objects: the role of hypersingular integral equations', in D. O. Thompson and D. E. Chimenti (eds.), *Review of Progress in Quantitative Nondestructive Evaluation*, Plenum Press, Brunswick, Maine, 1991.
13. Y. J. Liu, D. Zhang and F. J. Rizzo, 'Nearly singular and hypersingular integrals in the boundary element method', in: C. A. Brebbia and J. J. Rencis (eds.), *Boundary Elements XV*, Computational Mechanics Publications, Worcester, MA, 1993, pp. 453–468.
14. Y. J. Liu and F. J. Rizzo, 'Ultrasonic scattering from open cracks in 3-D using a composite boundary integral equation formulation', in D. O. Thompson and D. E. Chimenti (eds.), *Review of Progress in Quantitative Nondestructive Evaluation*, Plenum Press, New York, 1993, pp. 29–36.
15. Y. J. Liu and F. J. Rizzo, 'Scattering of elastic waves from thin shapes in three dimensions using the composite boundary integral equation formulation', *J. Acoust. Soc. Am.*, **102**(2), Pt. 1, August, 926–932 (1997).
16. F. J. Rizzo, 'An integral equation approach to boundary value problems of classical elastostatics', *Quart. Appl. Math.*, **25,** 83–95 (1967).
17. T. A. Cruse, 'Numerical solutions in three dimensional elastostatics', *Int. J. Solids Struct.*, **5,** 1259–1274 (1969).
18. T. A. Cruse, 'An improved boundary-integral equation method for three dimensional elastic stress analysis', *Comput. Struct.*, **4,** 741–754 (1974).
19. F. J. Rizzo and D. J. Shippy, 'An advanced boundary integral equation method for three-dimensional thermoelasticity', *Int. J. Numer. Meth. Engng.*, **11,** 1753–1768 (1977).
20. T. J. Rudolphi, 'The use of simple solutions in the regularization of hypersingular boundary integral equations', *Math. Comput. Modelling*, **15,** 269–278 (1991).

© 1998 John Wiley & Sons, Ltd.

21. Y. J. Liu and T. J. Rudolphi, 'Some identities for fundamental solutions and their applications to weakly-singular boundary element formulations', *Engng. Anal. Boundary Elements*, **8,** 301–311 (1991).
22. T. A. Cruse, *Boundary Element Analysis in Computational Fracture Mechanics*, Kluwer Academic Publishers, Dordrecht, Boston, 1988.
23. W. Lin and L. M. Keer, 'Scattering by a planar three-dimensional crack', *J. Acoust. Soc. Am.*, **82,** 1442–1448 (1987).
24. D. E. Budreck and J. D. Achenbach, 'Scattering from three-dimensional planar cracks by the boundary integral equation method', *J. Appl. Mech.*, **55,** 405–412 (1988).
25. G. Krishnasamy, T. J. Rudolphi, L. W. Schmerr and F. J. Rizzo, 'Hypersingular boundary integral equations: some applications in acoustic and elastic wave scattering', *J. Appl. Mech.*, **57,** 404–414 (1990).

.

 © 1998 John Wiley & Sons, Ltd.